Hindawi
International Journal of Corrosion
Volume 2020, Article ID 4045802, 14 pages
https://doi.org/10.1155/2020/4045802

Research Article

Electrochemical and Thermodynamic Investigation on Corrosion Inhibition of C38 Steel in 1M Hydrochloric Acid Using the Hydro-Alcoholic Extract of Used Coffee Grounds

Fatima Bouhlal,[1] Najoua Labjar ,[1] Farah Abdoun,[2] Aimad Mazkour,[3] Malika Serghini-Idrissi,[3] Mohammed El Mahi,[1] El Mostapha Lotfi,[1] and Souad El Hajjaji [3]

[1]*Laboratory of Spectroscopy, Molecular Modelling Materials, Nanomaterials, Water and Environment, CERNE2D, ENSET, Mohamed V University, Rabat, Morocco*
[2]*Center STIS, M2CS, ENSET, Mohammed V University, Rabat, Morocco*
[3]*Laboratory of Spectroscopy, Molecular Modelling, Materials, Nanomaterials, Water and Environment, CERNE2D, Faculty of Sciences, Mohamed V University, Rabat, Morocco*

Correspondence should be addressed to Najoua Labjar; najoua.labjar@um5.ac.ma

Received 22 May 2019; Revised 18 July 2019; Accepted 5 August 2019; Published 24 January 2020

Academic Editor: Ramazan Solmaz

The present work investigates the influence of temperature on C38 steel corrosion in a 1 M HCl medium with and without different concentrations of a hydro-alcoholic extract of used coffee grounds (HECG). The potentiodynamic polarization technique and the electrochemical impedance spectroscopy were performed in temperatures ranging from 293.15 to 323.15 K. It was observed that the inhibition efficiency decreased with increased temperature and inhibitor concentration. The HECG adsorption process on C38 steel surface was found to be spontaneous and obeyed to Langmuir isotherm at all studied temperatures. The associated thermodynamic parameters of adsorption led to suggest the occurrence of physical adsorption of the HECG compounds on the C38 steel surface.

1. Introduction

Corrosion inhibitors remain an original method to protect metals and their alloys against corrosion processes in corrosive environment [1, 2]. These are essentially organic molecules containing sulfur, oxygen, nitrogen, and phosphor. The inhibiting action of such compounds is mainly attributed to their adsorption on the metal surface [3, 4]. Additionally, The recent trend in metals protection is towards nontoxic inhibitors [5, 6].

Generally, coffee consumption generates large quantities of coffee residues [7, 8]. Based on the literature, used coffee grounds are rich in dietary fiber, protein, essential amino acids, and sugar [9]. Nevertheless, this waste is left with no apparent value in the industrial sector [10]. For these reasons, the use of this residue for metals protection against corrosion is an interesting ecofriendly solution.

Furthermore, it is commonly reported that temperature is one of the most significant factors that can influence the behavior of metals in an acidic environment, and can affect the metal-inhibitor interaction [4, 11]. Additionally, in acid medium, the metal corrosion rate increases with temperatures [12, 13]. Accordingly, a good understanding of corrosion behavior in such conditions is of great importance in the assessment of the corresponding risk factors [13, 14]. In fact, choosing appropriate inhibitors depends on parameters such as the type of acid, the temperature and the velocity of the fluid flow [15].

Several studies have investigated the effect of temperature on the inhibition of steel corrosion in acidic environments in the presence of green inhibitors [16, 17]. For instance, Ituen et al. [18] have studied the effect of temperature on the mild steel corrosion in 1 M H_2SO_4 in the presence of leaves and stems extracts of *Sida acuta*. Also, Afia et al. [19] have investigated the correlation between rising temperature and the anti-corrosive properties of Argan oil on C38 steel in 1 M HCl solution. Also, in another study, temperature effect on X70 steel corrosion

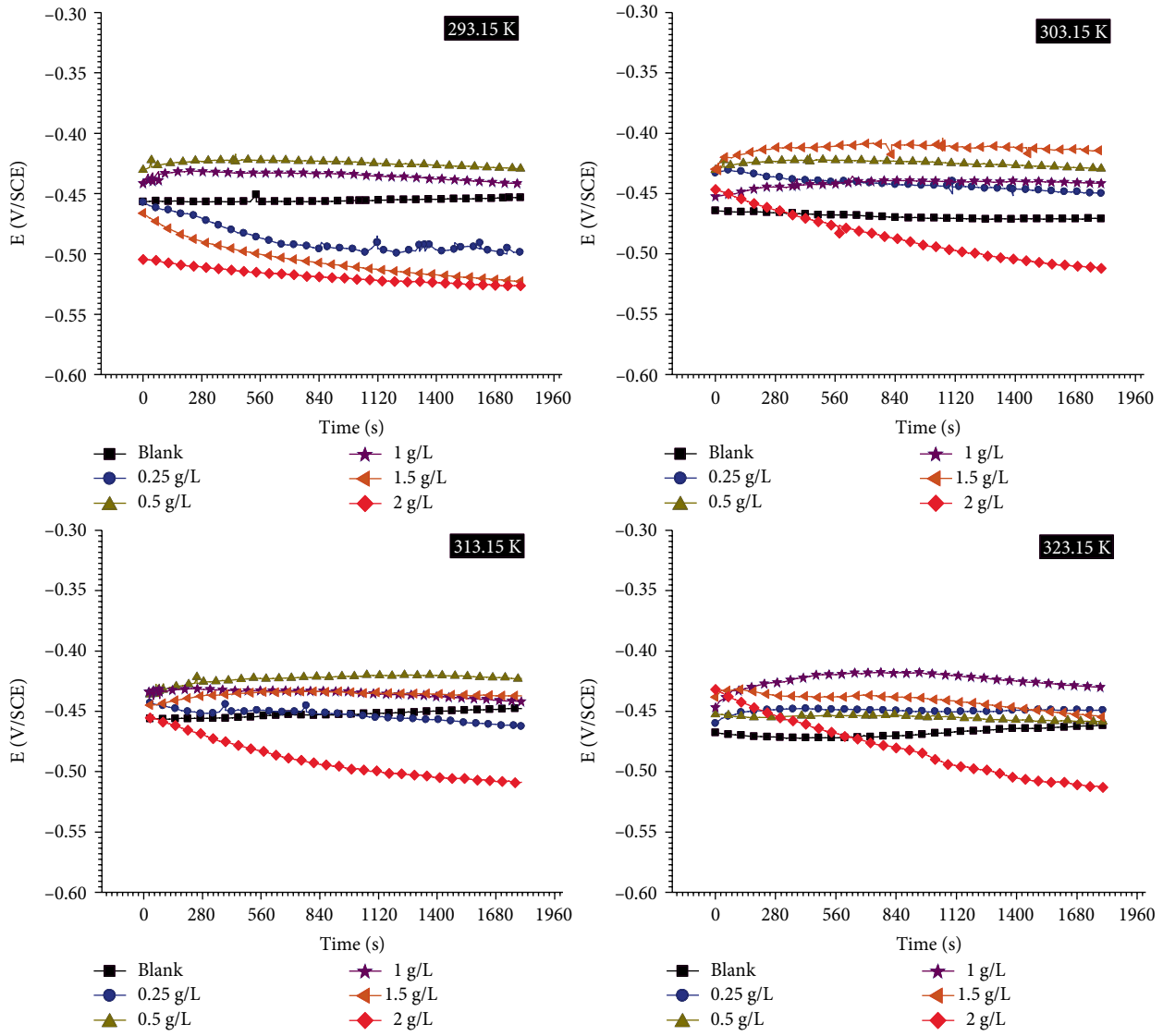

Figure 1: The evolution of open circuit potential (E_{OCP}) circuit potential as a function of immersion time in 1 M HCl.

Table 1: Chemical composition of C38 steel (wt.%).

Fe	C	Si	Mn	S	Cr	Ti	Co	Cu
98.39	0.37	0.23	0.68	0.016	0.077	0.059	0.009	0.16

inhibition by *Ginkgo* leaf extract in HCl solution has been carried out by Qiang et al. [20]. Li et al. [21] has assessed the inhibitory potential of *Ficus tikoua* leaves extract on C-steel corrosion in 1 M HCl media at varying temperatures.

On the other hand, the comparison of thermodynamic results obtained on the corrosion process in the presence and absence of inhibitors provides some conclusions regarding the inhibiting mechanism [22].

The present work focuses on the assessment of the inhibition performance of HECG in C38 steel corrosion under different temperatures and inhibitor concentrations. Various kinetic parameters for C38 steel corrosion in the absence and presence of the HECG were calculated and discussed.

2. Materials and Methods

2.1. Inhibitor Extraction. The used coffee grounds in this study were locally regularly taken from the same supplier. It is a blend of *Arabica* and *Robusta* coffees; which are the two most commonly consumed varieties of coffee in the world [12]. The used coffee grounds were put in the oven at 40°C in order to avoid any alteration during storage and also for drying.

The HECG was obtained by soxhlet extraction. 63 g of the solid was placed in a cartridge and then introduced into the soxhlet apparatus. In the flask, 300 mL of solvent (25% of the distilled water and 75% ethanol) was brought to a boil at a temperature of 78°C. When the solvent reaches the upper level of the siphon, the mixture was returned to the tank by pressure difference, where it was evaporated again and a new cycle starts again for a period of 5 hours.

Then, the final extract was recovered using a "rotavapor R-210". The extraction yield was determined using the following equation [23]:

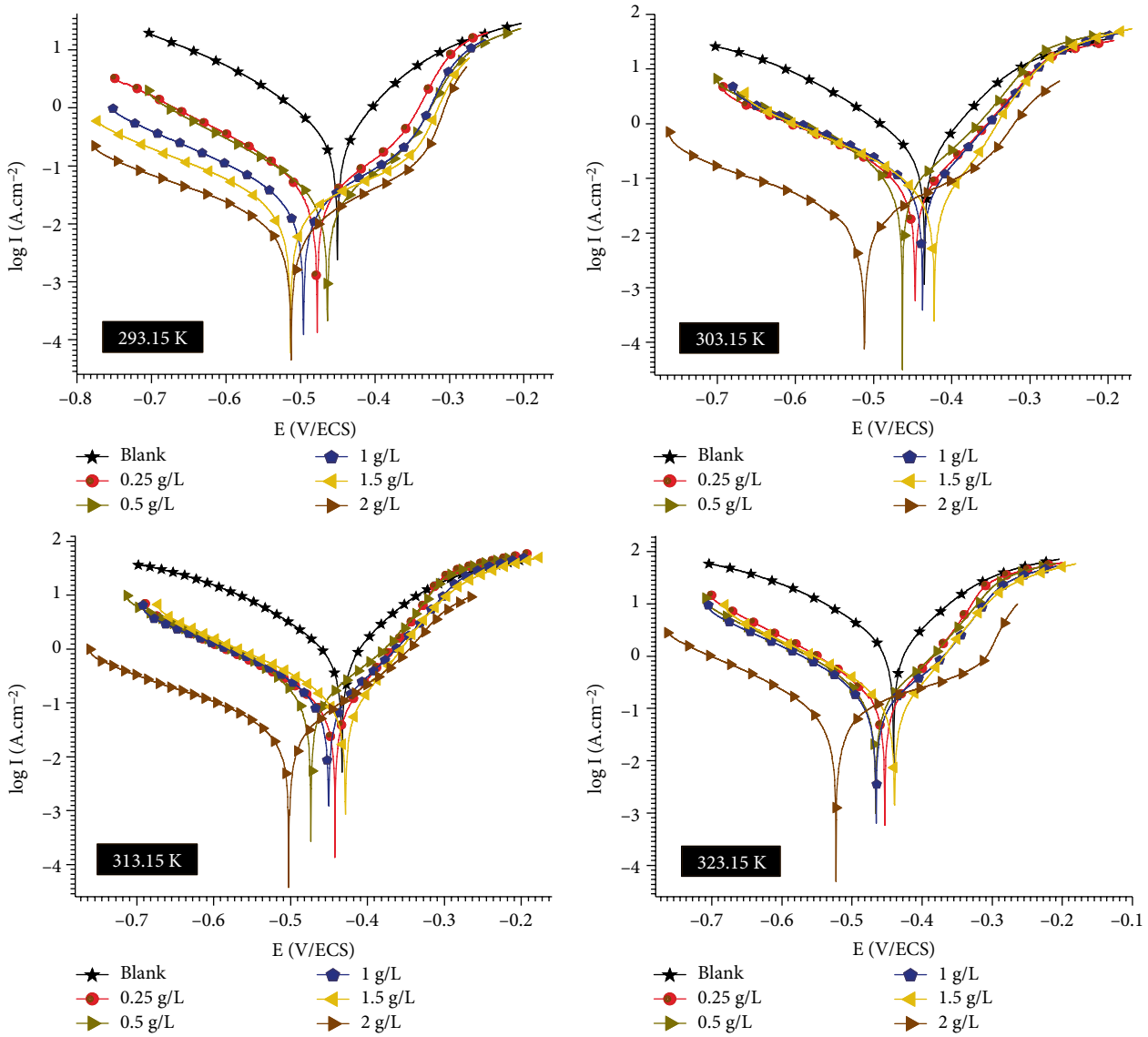

Figure 2: Effect of temperature on the cathodic and anodic curves of C38 steel in 1 M HCl with different concentrations of HECG.

$$Y = \frac{m_{ext}}{m_{ech}} \times 100, \quad (1)$$

where Y is the yield in %, m_{ext} is the mass of the extract after evaporation of the solvent in g and m_{ech} is the dry mass of the sample before extraction in g. The assays were performed in the concentration range from 0.25 to 2 g/L.

2.2. Material and Samples Preparation. The steel used in this work was a C38 carbon type with the chemical composition (wt.%) given in Table 1.

The exposed surface of working electrodes was abraded using a series of emery paper SiC (120–600 grade), followed by rinsing with distilled water, then degreased in acetone under ultrasound and then dried with hot air.

2.3. Electrochemical Assays. All electrochemical tests were carried out using a potentiostat "SP-150" piloted by EC-Lab software and in a Pyrex Cell equipped with a conventional three-electrode assembly. C38 steel has been used as working electrode (WE), saturated calomel electrode $Hg/Hg_2Cl_2/KCl$ (SCE) as reference electrode and platinum as an auxiliary electrode. The electrolyte was a 1 M HCl solution prepared from a commercial 37% HCl solution and distilled water. Tests were performed under varying temperatures from 293.15 to 323.15 K in 1 M HCl medium with and without different concentrations of the HECG after 30 min of immersion, in order to obtain a steady-state of the open circuit potential (E_{OCP}).

The anodic and cathodic polarization curves were plotted at a constant scan rate of 0.5 mV/s. The inhibition efficiency IE has been calculated according to the following equation:

$$IE = \frac{i_{corr,0} - i_{corr}}{i_{corr,0}} \times 100, \quad (2)$$

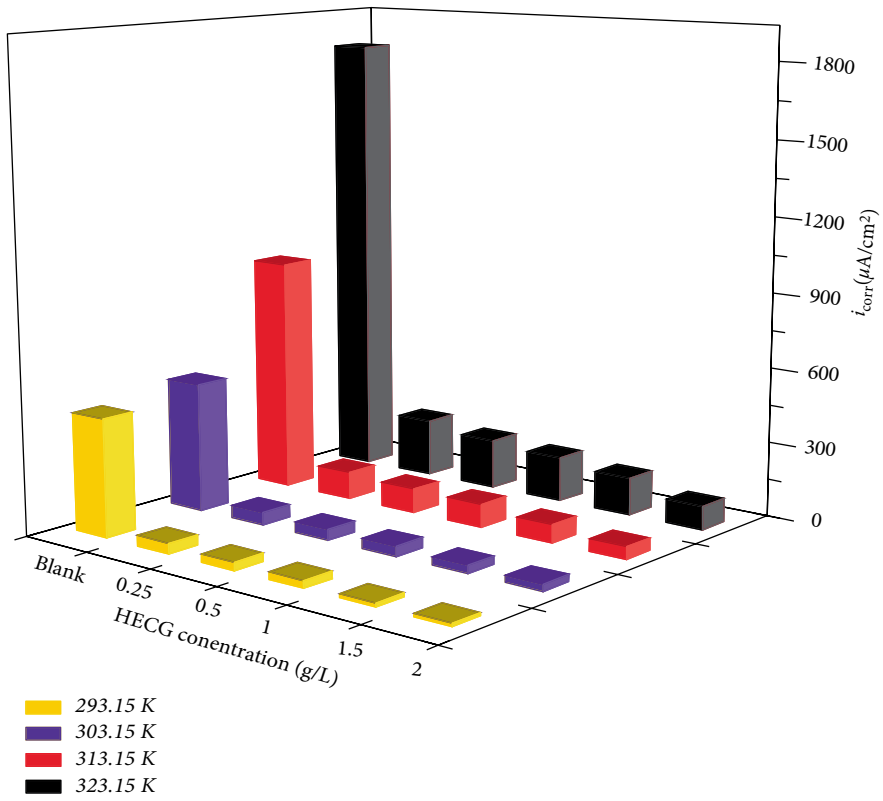

Figure 3: Variation of the corrosion current density with temperature and HECG concentration.

where i_{corr} and $i_{corr,0}$ are, respectively, the corrosion current density values of the steel determined by extrapolation of the cathode lines of TAFEL, with and without the addition of the inhibitor.

Electrochemical impedance measurements were performed after potential stabilization, applying a sinusoidal potential perturbation of 10 mV, in the frequency range from 100 kHz to 10 mHz with 6 points per decade. The inhibition efficiency IE has been determined using the following equation:

$$\mathrm{IE} = \frac{R_{ct} - R_{ct,0}}{R_{ct}} \times 100, \quad (3)$$

where R_{ct} and $R_{ct,0}$ are, respectively, the charge transfer resistance (R_{ct}) values of the steel with and without the addition of the inhibitor.

3. Results and Discussion

3.1. Open Circuit Potential (E_{OCP}) Measurements. Figure 1 shows the evolution of the open circuit potential according to immersion time during 30 minutes. The potential evolves towards stable values during the immersion time at each temperature and for all studied concentrations of HECG.

The E_{OCP} reaches quickly a steady-state condition after 30 minutes. Previous investigations reported similar behavior [15, 24]. All measured values are limited to a small range of potentials (between −0.52 V/ECS and −0.41 V/SCE) and only slight differences can be detected. There is no correlation between the variation of E_{OCP} and concentration. Indeed, the displacement of the HECG open circuit potential curves compared to that of the blank can indicate a mixed inhibition of corrosion, in agreement with the results of Torres et al. [25].

3.2. Potentiodynamic Polarization Assay. The potentiodynamic polarization was performed in order to assess the temperature effect on the inhibition performance of the HECG on C38 steel corrosion. The experiments were conducted at different temperatures (293.15–323.15 K) in 1 M HCl without and with different concentrations of the HECG (Figure 2).

From Figure 2, the addition of the HECG inhibitor leads to an inhibition of both cathodic and anodic reactions. This supports the fact that the HECG inhibits C38 steel corrosion by controlling both anodic and cathodic reactions (mixed type inhibitor) [26, 28]. Nonetheless, a negative displacement of the corrosion potentials, compared to the blank solution, has occurred [29]. This may be explained by the adsorption of the inhibitor molecules on active sites, thereby reducing the reduction of H^+ ions [4].

In the anodic domain, the potential moves positively above a specific value, the inhibitor desorption begins to occur. This potential can be defined as the desorption potential [30]. This also indicates that the desorption rate of HECG is greater than the one of adsorption for such potentials [31]. In addition, at higher temperatures, the inhibitor desorption started at more

Table 2: Electrochemical parameters of C38 steel in 1 M HCl at different temperature and with different concentrations of HECG.

T(K)	C (g/L)	$-E_{corr}$ (mV/SCE)	$-\beta_c$ (mV)	β_a (mV)	i_{corr} (μA/cm^2)	IE (%)	θ
293.15	Blank	467.56	165.1	107.7	471.84	—	—
	0.25	477.53	123.4	142.3	41.16	91.27	0.91
	0.5	463.793	132.9	139.3	32.62	93.08	0.93
	1	495.877	172.4	185.1	29.34	93.78	0.93
	1.5	468.165	142.7	114.6	14.88	96.84	0.96
	2	512.528	244.5	200.7	12.42	97.36	0.97
303.15	Blank	434.966	186.6	114.5	617.13	—	—
	0.25	463.368	104.3	85.4	67.89	88.99	0.89
	0.5	437.249	119.3	71.9	60.00	90.27	0.90
	1	446.862	112.9	74.4	57.40	90.69	0.90
	1.5	422.386	94.9	51.3	34.99	94.33	0.94
	2	483.017	129.1	117.0	29.98	95.14	0.95
313.15	Blank	433.281	131.0	98.7	989.88	—	—
	0.25	473.608	104.8	97.3	116.06	88.27	0.88
	0.5	428.600	131.9	69.9	97.98	90.10	0.90
	1	450.438	117.7	85.3	96.09	90.29	0.90
	1.5	442.139	107.2	58.0	62.95	93.64	0.93
	2	501.132	198.6	222.4	60.00	93.93	0.93
323.15	Blank	440.487	129.1	105.1	1 794.01	—	—
	0.25	453.151	156.9	101.5	230.14	87.17	0.87
	0.5	466.388	136.7	110.0	198.26	88.94	0.88
	1	439.245	158.0	91.8	179.23	90.00	0.90
	1.5	465.691	129.1	115.6	150.26	91.62	0.91
	2	512.063	288.3	444.0	130.65	92.71	0.92

negative potentials compared to that of 393.15 K. This confirms that the corrosion of C38 steel in 1 M HCl is significantly enhanced when the temperature increases [32–34]. After the desorption potential, the plots become almost similar to the blank one. This was found to occur for all studied temperatures and all inhibitor concentrations.

Figure 3 illustrates the temperature dependence of C38 steel corrosion in 1 M HCl solution in the presence of different concentrations of the HECG.

The electrochemical parameters obtained from the polarization curves are listed in Table 2.

From Table 2 and Figure 3, it can be observed that the inhibition efficiency of HECG rises with increasing concentration and significantly decreases with increasing temperature, for both uninhibited and inhibited solutions. By increasing the temperature, the aggressiveness of the corrosive medium is expected to increase. Accordingly, the inhibition efficiency decreases [4, 11]. This may be an indication of the physical adsorption mechanism of HECG on the metal surface [35]. Nevertheless, HECG could continue to strongly adsorb and serve as an effective corrosion inhibitor for C38 steel. IE was maintained at 92.71% with 2 g/L HECG at a temperature of 323.15 K.

3.3. Electrochemical Impedance Spectroscopy (EIS). The electrochemical impedance spectroscopy was performed to investigate the effect of the temperature and inhibitor concentration on the impedance behavior of C38 steel in 1 M HCl solution. The Nyquist and the corresponding Bode plots are presented in Figures 4 and 5, respectively.

The global form of the Bode diagrams is generally similar in both cases (with and without inhibitor); it is the same for all concentrations and all studied temperatures. This indicates that the addition of the inhibitor does not induce any change in the corrosion mechanism [36]. From Figure 4 one time constant was observed for all concentrations and temperatures except for the concentration of 2 g/L, two time constants were noticed at 313.15 and 323.15 K. Additionally, it can be clearly seen that the maximum phase angle increases with the rise of HECG concentration, which may be due to the inhibitor's adsorption on the steel surface [37]. A linear relationship between log $|Z|$ versus log ($freq$) has also been noted. Table 3 shows the values of the slopes of the Bode plots at intermediate frequencies, the maximum phase angles (θ_{max}) and the corresponding frequencies ($freq_{ma}$) for C38 steel in 1 M HCl solution containing different concentrations of HECG at different temperatures.

From Table 3, we noticed that the slopes of the Bode plots at intermediate frequencies ranging from −0.3 to −4.1 and maximum phase angles (θ_{max}) ranging from 35° to 69°. These deviations of the slopes and θ_{max} from the ideal values of −s1 and −90°, respectively, can be considered as the deviation from the ideal capacitive behavior [30].

At each temperature, the frequency range with the maximum phase angle widened as the inhibitor concentration rose. These results supported the inhibition ability of the HECG studied for corrosion of C38 steel in HCl 1 M medium [27].

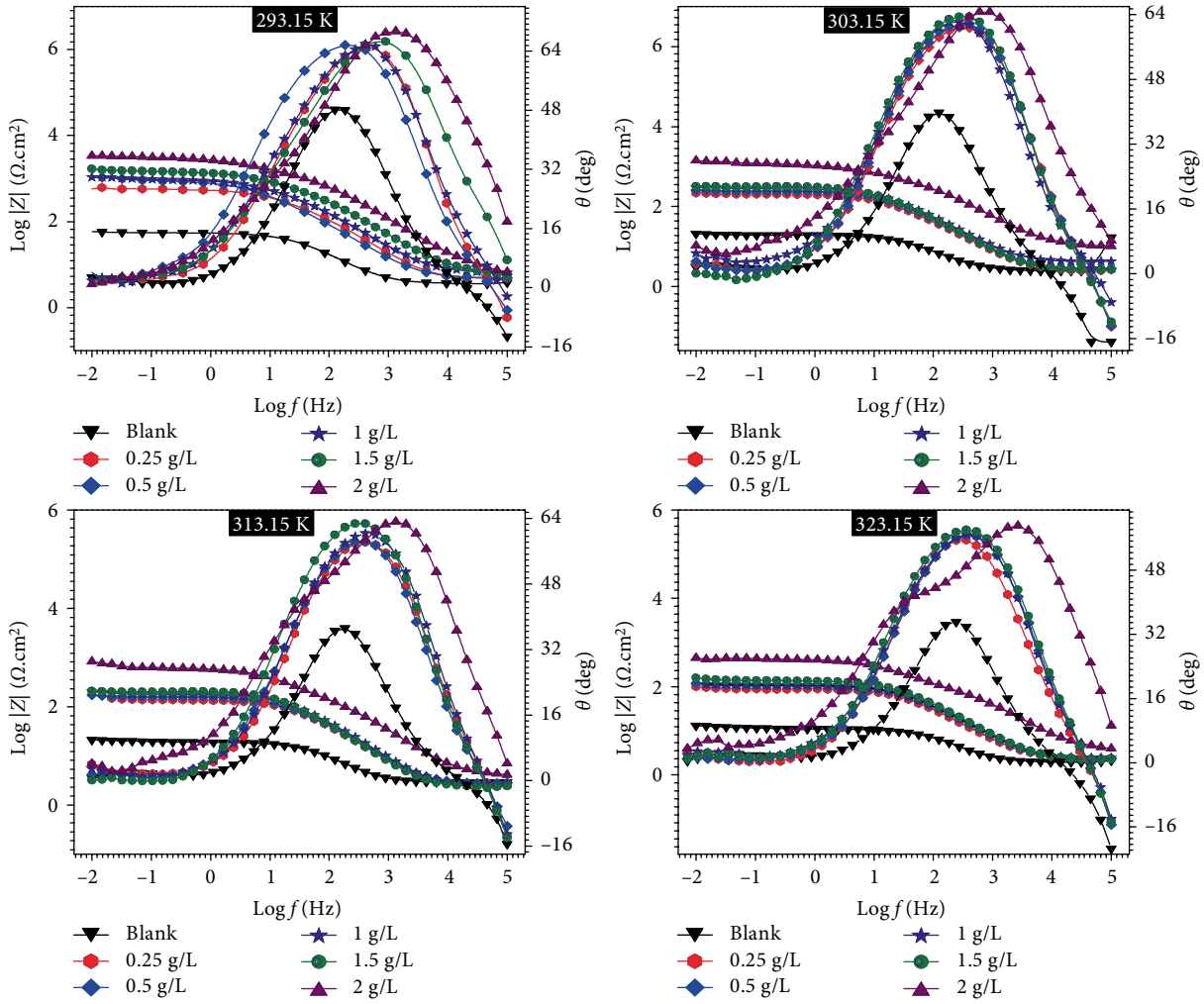

Figure 4: Bode graphs of the measured impedance.

The Nyquist diagrams obtained consist of the depressed semi-circle, which indicates that the steel dissolution is essentially a charge transfer process [38].

The size of the Nyquist plots rises with respect to the blank solution and with increasing HECG concentration signifying that the HECG compounds formed an inhibitor film on the C38 steel surface. Moreover, a decrease in the size of the capacitive loops as the temperature increase was observed. This behavior implies that an increase in temperature accelerates the corrosion process [27].

All the spectra were well modeled using a time constant shown in Figure 6(a), excluding the concentration 2 g/L in both temperatures 303.15 and 323.15 K. In the last case, a second time constant was added to the equivalent circuit used (Figure 6(b)) to adjust the experimental points. The electrical parameters determined from the adjustment of the experimental data are collected in Table 4.

In this model, R_1 represents the resistance of the solution, placed in series with the resistance due to the film formed on the steel surface (R_2); R_3 is the resistance of the faradic reaction. Q_1, Q_2, and Q_3 are the constant phase elements representing the capacity of the double layer at the metal/solution interface. Generally, there is a phase shift between "Q" and "pure capacity". Therefore, the simulation of impedance spectra can be performed by replacing the capacitor C with a constant phase element (CPE). The impedance of the CPE is described by the following equation [39]:

$$Z(\mathrm{Qc}) = Y_0^{-1}(j\omega)^{-n}, \tag{4}$$

where Y_0 is the general induction function, j denotes the complex operator, ω denotes the angular frequency (in rad.s^{-1}) and n denotes the coefficient related to the phase shift which can be explained by the degree of homogeneity of the metal surface ($0 < n \leq 1$), $n = 1$ when the CPE is reduced to an ideal capacitor (C) [40].

The CPE was introduced into the circuit, in order to take into account the nonideal behavior due to the phenomena of inhomogeneity, roughness, porosity, and adsorption on the C38 steel surface. The C_{dl} value can be calculated using the following equation [27]:

$$C = Y_0(\omega_{\max})^{n-1}, \tag{5}$$

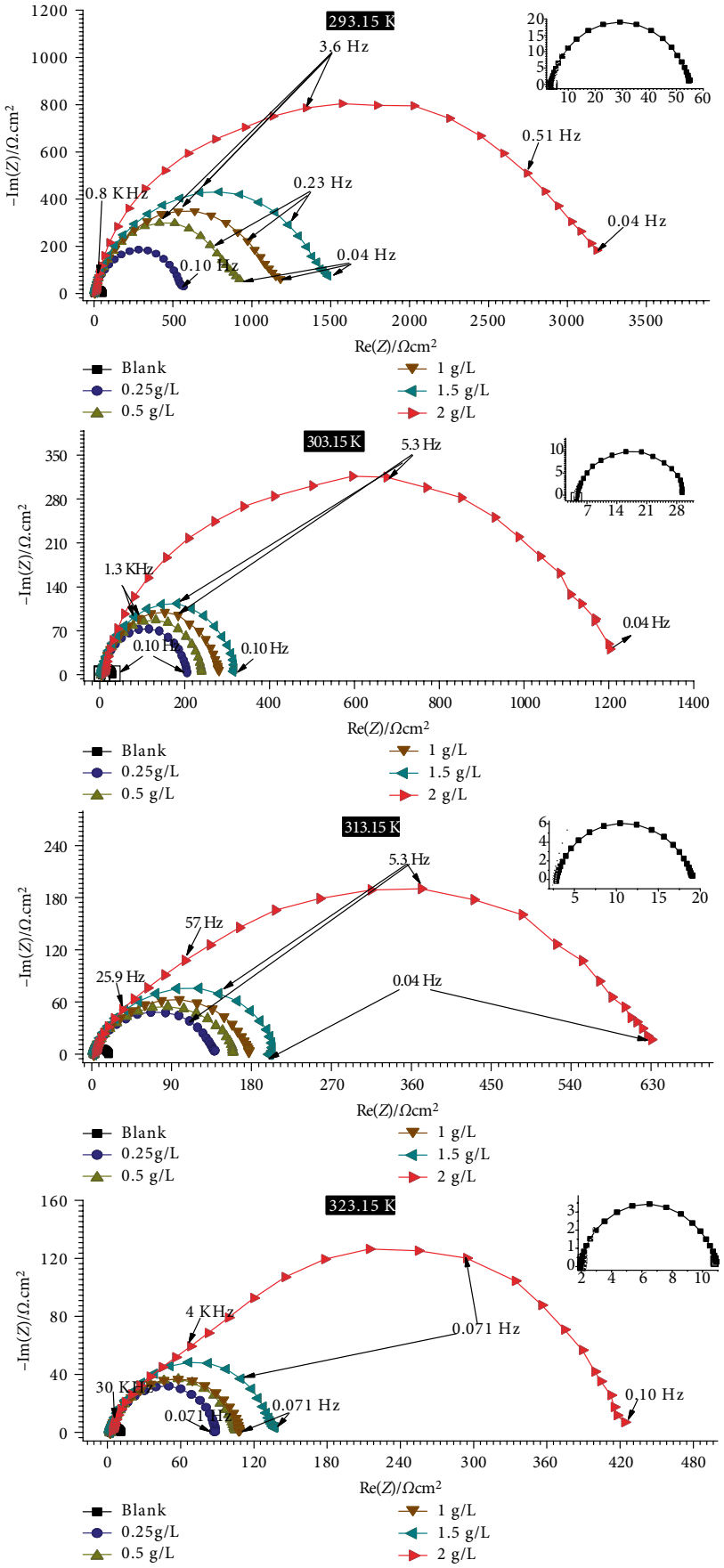

Figure 5: Nyquist plots obtained for C38 steel in 1 M HCl with different temperatures and inhibitor concentrations.

Table 3: Slopes of the Bode plots at intermediate frequencies, the maximum phase angles (θ_{max}) and the corresponding frequencies ($freq_{max}$) for C38 steel in 1 M HCl solution containing different concentrations of HECG at different temperatures.

Temperature (K)	C (g/L)	θ_{max} (deg)	$freq_{max}$	Slope
293.15	Blank	48.10	2.09	−0.52
	0.25	65.09	2.60	−0.75
	0.5	65.60	2.26	−0.74
	1.0	65.90	2.60	−0.74
	1.5	66.59	2.60	−0.72
	2	69.34	3.12	−0.70
303.15	Blank	46.69	0.32	−2.94
	0.25	60.83	0.38	−3.64
	0.5	61.76	0.416	−3.72
	1.0	62.17	0.38	−3.86
	1.5	63.44	0.416	−3.68
	2	64.67	0.47	−3.18
313.15	Blank	37.19	0.35	−2.29
	0.25	58.18	0.41	−3.83
	0.5	58.38	0.41	−3.85
	1.0	60.27	0.41	−3.93
	1.5	62.69	0.41	−4.13
	2	63.16	0.49	−3.48
323.15	Blank	35.09	2.43	−0.32
	0.25	55.56	2.60	−0.54
	0.5	56.78	2.60	−0.54
	1.0	56.94	2.60	−0.53
	1.5	58.10	2.60	−0.57
	2	59.09	3.46	−0.43

where $\omega_{max} = 2\pi f_{max}$ and f_{max} is the frequency at the maximum value of the imaginary component of the impedance spectra.

The results obtained by adjusting the electrical parameters using these electrical circuits are presented in Table 4.

The uncompensated resistance at high frequency, which corresponds to the resistance of the electrolyte, seems to be slightly affected by the addition of the HECG, which indicates that the extract used meets the requirement of being reliable without changing the physicochemical parameters of the solution. Besides, the addition of the HECG induces a simultaneous increase in resistance film and that of the faradic reaction, which shows the protective effect of the extract against C38 steel corrosion. The decline in the capacity as the concentration of HECG rises can lead to a decrease in the dielectric constant and consequently an increase in the thickness of the double layer, in accordance with Helmholtz's model [25] as follows:

$$C_{dl} = \frac{\varepsilon \varepsilon_0 A}{\delta}, \tag{6}$$

where ε is the dielectric constant of the medium, ε_0 is the vacuum permittivity, A is the electrode surface area and δ is the thickness of the protective layer. This suggests that the HECG molecules gradually replace the water molecules and other ions initially adsorbed to the surface.

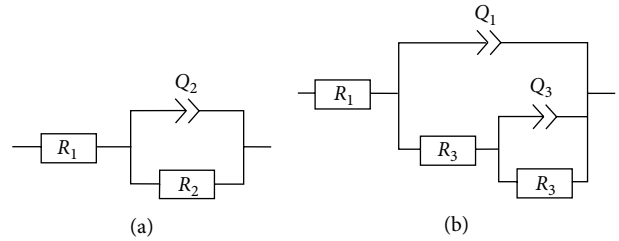

Figure 6: Equivalent circuits used to fit the EIS experimental data.

All the findings above indicate the decreasing of inhibition efficiency of HECG with temperature, which can be attributed to the desorption of the adsorbed inhibitor molecules as a result of increased thermal agitation. Consequently, the roughness of the metal surface increases, which can also reduce the ability of the inhibitor to be adsorbed on the metal surface [42].

3.4. Adsorption Isotherm and Mechanism of Corrosion Inhibition. It was previously reported that the interaction between inhibiting molecules and the metallic surface is a primary factor in determining the effectiveness of an inhibitor [43, 44]. Different adsorption isotherms including Temkin, Frumkin, and Langmuir were, therefore, tested to adjust the data obtained from polarization curves.

We have found that the Langmuir isotherm gives the best fit (Figure 7), with a correlation coefficient $R^2 = 0.99$. This suggests that the adsorption of HECG on the C38 steel surface, obeys the Langmuir isotherm, which can be represented as follows [45, 46]:

$$\frac{C_{inh}}{\theta} = \frac{1}{K_{ads}} + C_{inh}, \tag{7}$$

where θ is the surface coverage, $\theta = (IE/100)$, C_{inh} is the inhibitor concentration in the electrolyte and K_{ads} the equilibrium constant of the adsorption process, representing the degree of adsorption.

The Langmuir isotherm assumes that the metal surface contains a fixed number of active sites and each inhibitor molecule occupies a single active site [47, 48].

As reported, the adsorption equilibrium constant (K_{ads}), and the standard adsorption free energy $\left(\Delta G^0_{ads}\right)$are the primary adsorption factors in corrosion inhibition investigations [49, 50]. These two parameters are linked by the following equation [39]:

$$K_{ads} = \frac{1}{55.5} \exp\left(\frac{-\Delta G^0_{ads}}{RT}\right), \tag{8}$$

where R is the molar gas constant, T is the absolute temperature and 55.5 is the molar concentration of water in mol.l^{-1}.

The adsorption parameters obtained from Langmuir isotherm adjustment are shown in Table 5.

As reported in Table 5 and according to the results reported by Qiang et al. [27] and Alaneme et al. [17], the K_{ads} values decrease with temperature, which implies an intensification

Table 4: Electrical parameters and inhibitory effectiveness of C38 steel corrosion in 1 M HCl solution containing different concentrations of the extract.

T (K)	C (g/L)	R_1 (Ω cm^2)	Q_1 (e^{-3} F cm^{-2})	n_1	R_2 (Ω cm^2)	Q_3 (e^{-3} F cm^{-2})	n_3	R_3 (Ω cm^2)	R_{ct} (Ω cm^2)	IE
293.15	Blank	3.626	0.31	0.816	51.54	/	/	/	51.54	—
	0.25	3.42	0.09	0.76	556.3	/	/	/	556.3	90.73
	0.5	4.081	0.08	0.76	906.5	/	/	/	906.5	94.31
	1	1.748	0.06	0.69	1180	/	/	/	1180	95.63
	1.5	3.341	0.03	0.69	1475	/	/	/	1 475	96.50
	2	1.004	0.02	0.64	3272	/	/	/	3 272	98.42
303.15	Blank	3.31	0.36	0.83	36.83	/	/	/	24.9	
	0.25	2.03	0.13	0.78	207	/	/	/	207	87.97
	0.5	2.37	0.12	0.78	246	/	/	/	246	89.87
	1	3.612	0.12	0.78	281.8	/	/	/	281.8	91.16
	1.5	2.375	0.12	0.78	322.2	/	/	/	322.2	92.27
	2	2.733	0.05	0.63	1222	/	/	/	1 222	97.96
313.15	Blank	2.82	0.56	0.81	16.29	/	/	/	16.29	
	0.25	2.35	0.14	0.78	135	/	/	/	135	87.93
	0.5	2.541	0.14	0.78	158.6	/	/	/	158.6	89.72
	1	2.24	0.12	0.77	177	/	/	/	177	90.79
	1.5	2.22	0.12	0.8	207.3	/	/	/	207.3	92.14
	2	3.266	0.06	0.71	46.41	0.02	0.5	590.8	637.21	97.44
323.15	Blank	3.01	0.61	0.8	10.9	/	/	/	10.9	
	0.25	2.248	0.16	0.80	86.95	/	/	/	86.95	87.46
	0.5	2.06	0.16	0.77	103.4	/	/	/	103.4	89.45
	1	2.37	0.16	0.78	107	/	/	/	107.2	89.83
	1.5	2.19	0.13	0.79	134.4	/	/	/	134.4	91.88
	2	3.89	0.02	0.79	133.2	0.007	0.8	282.7	415.9	97.37

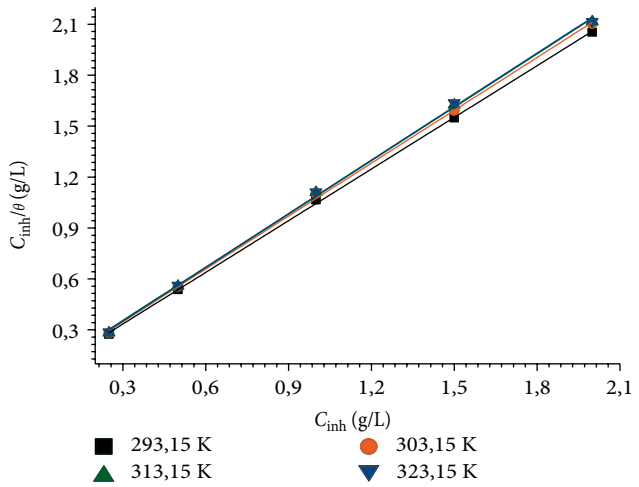

Figure 7: Langmuir adsorption isotherm of HECG on C38 steel in 1 M HCl at different temperatures.

of corrosion, thus limiting the ability of the inhibitor to adsorb on the C38 steel surface.

Negative values of the standard free adsorption energy, as shown in Table 5 refer to the spontaneous adsorption of the extract compounds on the C38 steel surface [51, 52]. The absolute values of ΔG^0_{ads} lated are less than 20 kJ mol^{-1}, meaning

Table 5: Langmuir isotherm parameters for the adsorption of HECG on the C38 steel surface.

Temperature (K)	Slope	K_{ads} (M^{-1})	$-\Delta G^0_{ads}$ (kJ/mol)	R^2
293.15	1.01	33.57	18,35	0.99
303.15	1.03	28.29	18.54	0.99
313.15	1.04	27.70	19.10	0.99
323.15	1.04	24.92	19.43	0.99

that the inhibitor adsorption on the metallic surface occurred, generally, by a physical adsorption mechanism [38, 53]. This kind of adsorption implies electrostatic interaction between a charged molecule and a charged metal, which is highly sensitive to thermal agitation and easily breaks as the latter rises [35], this supports the conclusion that the inhibition efficiency decrease with increasing temperature.

For the inhibition mechanism, in hydrochloric acid medium, the mechanism proposed for the corrosion of C38 steel by other authors and which seems to be the most adequate for the cathodic reaction of hydrogen release includes the following steps [40]:

$$Fe + H^+ \leftrightarrow (FeH^+)_{ads}, \quad (9)$$

$$(FeH^+)_{ads} + e^- \leftrightarrow (FeH)_{ads}, \quad (10)$$

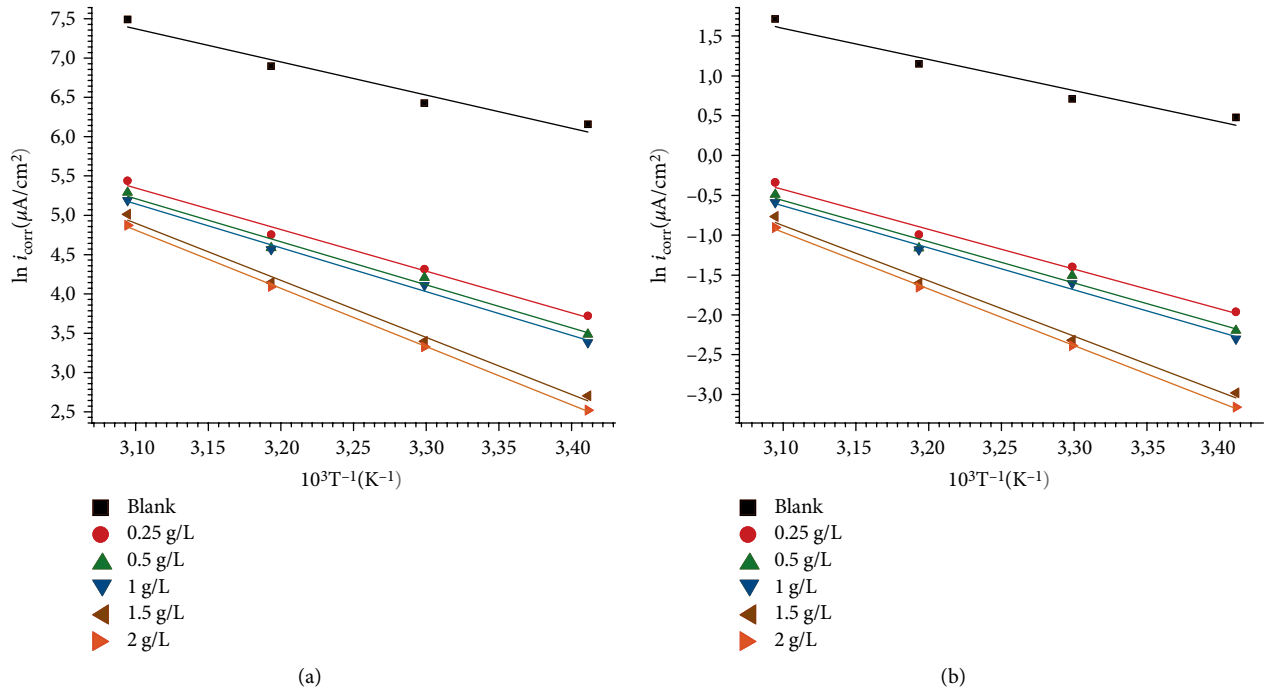

Figure 8: (a) Arrhenius plots, (b) transition state plots for C38 steel in 1 M HCl without and with different concentration of HECG.

$$(FeH)_{ads} + H^+ + e^- \leftrightarrow Fe + H_2. \quad (11)$$

Similarly, the proposed dissolution mechanism for the anodic reaction involving the role of chloride ions in this process is as follows [54]:

$$Fe + Cl^- \leftrightarrow (FeCl^-)_{ads}. \quad (12)$$

$$(FeCl^-)_{ads} \leftrightarrow (FeCl)_{ads} + e^-. \quad (13)$$

$$(FeCl)_{ads} \leftrightarrow\rightarrow (FeCl^+) + e^-. \quad (14)$$

$$FeCl^+ \leftrightarrow Fe^{2+} + Cl^-. \quad (15)$$

According to the detailed mechanism above, the displacement of some adsorbed Cl^- water molecules on the metal surface by the inhibitor species to yield the adsorbed intermediate $(FeCl^-)_{ads}$ reduces the amount of the species $(FeCl^+)_{ads}$ available for the rate-determining steps and consequently retards Fe anodic dissolution [56].

3.5. Thermodynamic Parameters. The assessment of thermodynamic parameters is of great importance in the analysis of the adsorption of inhibitors on the metal surface [4, 57].

The plots of i_{corr} and i_{corr}/T as a function of reciprocal of the temperature were fitted well and are illustrated in Figure 8.

The thermodynamic parameters for the studied system were estimated using the following equations [58, 59]:

$$i_{corr} = Ke^{(-E_a/RT)}, \quad (16)$$

where E_a is the activation energy and K = Arrhenius constant

Table 6: Thermodynamic parameters.

Concentration	ΔH_a^0 (kJ.mol^{-1})	$-\Delta S_a^0$ (J.mol^{-1})	E_a (kJ/mol)
Blank	32.51	83.36	35.07
0.25 g/L	41.48	72.39	44.03
0.5 g/L	43.02	68.76	45.57
1 g/L	43.81	66.87	46.36
1.5 g/L	57.81	25.51	60.36
2 g/L	59.04	22.43	61.59

$$i_{corr} = \frac{RT}{Nh}\exp\left(\frac{\Delta S_a^0}{R}\right)\exp\left(-\frac{\Delta H_a^0}{RT}\right), \quad (17)$$

N, h, ΔS_a^0, and ΔH_a^0 are the Avogadro number, the Planck constant, the entropy the activation enthalpy, respectively.

The results are presented in Table 6.

The plots of $\ln(i_{corr})$ vs. $1/T$ and $\ln(i_{corr}/T)$ vs. $1/T$ gave straight lines with linear regression coefficients were close to unity for all the inhibitor concentration studied.

The parameters in Table 6 revealed that the apparent activation energy values, E_a for the blank solution is 35.07 kJ.mol^{-1} and in the presence of the HECG ranges from 44.03 to 61.59 kJ.mol^{-1}. It is evident that activation energy is higher in inhibited solution than in the blank one.

According to Mobin and al. [60]; Karthikaiselvi and al. [61], the higher E_a value in presence of inhibitor indicates physical adsorption mechanism of the inhibitor on the steel surface. The increase in E_a value can also be attributed to a noticeable decrease in the adsorption of the inhibiting molecules on the metallic surface with an increase in temperature [62]. This suggests that the energy barrier of the

Table 7: Different investigated coffee extracts as an inhibitor for steel corrosion in 1 M HCl medium.

Inhibitor	Concentration (g/L)	Inhibition efficiency (%)	Inhibitor type	Reference
Aqueous roasted coffee extract	1	84	Mixed	[69]
Coffee husk aqueous extract	0.5	84.1	Mixed	[68]
Aqueous coffee ground extract	0.4	88.1	Mixed	[25]
Hydro-alcoholic extract of used coffee grounds	0.25	91	Mixed	Present work

corrosion reaction rises in the presence of the HECG [63, 64].

The positive sign of the enthalpy values is principally associated with endothermic nature of the corrosion process of C38 steel, meaning the slow dissolution of C38 steel in the presence of the HECG [64, 65].

As reported in Table 6, the negative increase in ΔS_a^0 values reflects that velocity represents an association rather than a dissociation step. This implies that a decrease in disorder occurs when reagents are transferred to the activated complex [28, 64].

It is important to indicate that the adsorption mechanism of natural product extracts explanation is complicated. This is due to the ignorance of the molecular structure and number of the chemical components in the extract. Some authors [36, 48, 66], in their study on acidic corrosion media with extracts, reported the same limitation. Notwithstanding this limitation, the present study can strongly state that corrosion of C38 steel is inhibited by the addition of inhibitor in HCl 1 M medium and also that inhibiting efficiency decreases with increasing temperature.

Many studies report that in acid concentrations, more or less close to 1 M, extracts of natural products are known as effective inhibitors that act mainly as mixed type corrosion inhibitors [67, 68]. In fact, natural products are rich with compounds, which can interact with a metal surface and block anodic and cathodic corrosion mechanism. These compounds are mainly, organic sugars, alkaloids, tannins, polyphenols, flavonoids, …etc. [67].

Torres et al. [25] have highlighted the higher level of antioxidant components in the aqueous coffee ground extract which indicates that it is a suitable candidate for inhibiting carbon steel corrosion. Moreover, the hydro-alcoholic extract of used coffee grounds is a competitive inhibitor with a high inhibition efficiency compared to other extracts (Table 7), which may be due to the extraction method and the polarity of the solvent used.

It is to be noted that the great inhibition effectiveness of coffee residue extracts is obviously an excellent opportunity to recycle this type of residue, which has been considered as waste [68].

Table 7 lists different coffee extracts used as an inhibitor for steel corrosion in 1 M HCl medium.

4. Conclusion

The following results can be drawn from this study:

(i) The inhibition efficiency values increased with increasing HECG concentration and decreased with temperature.

(ii) The results obtained from the potentiodynamic polarization indicate that HECG has affected anodic and cathodic reactions, allowing a mixed-type inhibition by a simple blockage of the active sites on the metal.

(iii) The Langmuir adsorption isotherm was found to better describe the experimental results reported in this study. In the same way, the thermodynamic parameters obtained from this study indicate that the presence of the HECG increases the activation energy, and the negative value of $-\Delta G_{ads}^0$ is a sign of spontaneous adsorption of the HECG species on the C38 steel surface.

Nevertheless, HECG has a great potential as a C38 steel corrosion inhibitor with an important efficiency value of 92.71%, with a concentration of 2 g/L at 323.15 K.

Data Availability

The data used to support the findings of this study are available from the corresponding author upon request.

Conflicts of Interest

The authors declare that they have no conflicts of interest.

Acknowledgments

We thank Karimi Lamiae, Researcher at Laboratory of Space and Culture, and faculty of Letters and Humanities, Mohamed Premier University Oujda for participating in the language review.

References

[1] N. M'hiri, D. Veys-Renaux, E. Rocca, I. Ioannou, N. M. Boudhrioua, and M. Ghoul, "Corrosion inhibition of carbon steel in acidic medium by orange peel extract and its main antioxidant compounds," *Corrosion Science*, vol. 102, pp. 55–62, 2016.

[2] B. Zhang, C. He, C. Wang, P. Sun, and F. Li, "Synergistic corrosion inhibition of environment-friendly inhibitors on the

corrosion of carbon steel in soft water water," *Corrosion Science*, vol. 94, pp. 6–20, 2015.

[3] M. E. Mert, G. Kardas, and B. Yazıcı, "Experimental and theoretical investigation of 3-amino-1 , 2 , 4-triazole-5-thiol as a corrosion inhibitor for carbon steel in HCl medium," *Corrosion Science*, vol. 53, no. 12, pp. 4265–4272, 2011.

[4] T. Douadi, H. Hamani, D. Daoud, M. Al-noaimi, and S. Chafaa, "Effect of temperature and hydrodynamic conditions on corrosion inhibition of an azomethine compounds for mild steel in 1 M HCl solution," *Journal of the Taiwan Institute of Chemical Engineers*, vol. 71, pp. 388–404, 2017.

[5] N. El Hamdani, R. Fdil, M. Tourabi, C. Jama, and F. Bentiss, "Alkaoids extract of *Retama monosperma* (L.) boiss. Seeds used as novel eco-freindly ihnibitor for carbon steel corrosion in 1 M HCl solution," *Applied Surface Science*, vol. 357, pp. 1294–1305, 2015.

[6] R. T. Loto and C. A. Loto, "Anti-corrosion properties of the symbiotic effect of Rosmarinus officinalis and trypsin complex on medium carbon steel," *Results in Physics*, vol. 10, pp. 99–106, 2018.

[7] L. F. Ballesteros, J. A. Teixeira, and S. I. Mussatto, "Extraction of polysaccharides by autohydrolysis of spent coffee grounds and evaluation of their antioxidant activity," *Carbohydrate Polymers*, vol. 157, pp. 258–266, 2017.

[8] Y.-F. Shang, J.-I. Xu, W.-J. Lee, and B.-H. Um, "Antioxidative polyphenolics obtained from spent coffee grounds by pressurized liquid extraction extraction," *South African Journal of Botany*, vol. 109, pp. 75–80, 2017.

[9] J. C. Page, N. P. Arruda, and S. P. Freitas, "Crude ethanolic extract from spent coffee grounds: volatile and functional properties," *Waste Management*, vol. 69, pp. 463–469, 2017.

[10] J. Simões, F. M. Nunes, M. R. Domingues, and M. A. Coimbra, "Extractability and structure of spent coffee ground polysaccharides by roasting pre-treatments," *Carbohydrate Polymers*, vol. 97, no. 1, pp. 81–89, 2013.

[11] I. B. Obot and N. O. Obi-egbedi, "Adsorption properties and inhibition of mild steel corrosion in sulphuric acid solution by ketoconazole: experimental and theoretical investigation," *Corrosion Science*, vol. 52, no. 1, pp. 198–204, 2010.

[12] D. Bouknana, B. Hammouti, M. Messali, A. Aouniti, and M. Sbaa, "Olive pomace extract (OPE) as corrosion inhibitor for steel in HCl medium," *Asian Pacific Journal of Tropical Disease*, vol. 4, pp. S963–S974, 2014.

[13] R. Geethanjali, R. Menaka, and S. Subhashini, "Gravimetric and electrochemical study of temperature effect of PVA grafted terpolymer on corrosion inhibition of mild steel in hydrochloric acid," *Materials Today Proceedings*, vol. 5, no. 8, pp. 16246–16257, 2018.

[14] A. Popova, "Temperature effect on mild steel corrosion in acid media in presence of azoles," *Corrosion Science*, vol. 49, no. 5, pp. 2144–2158, 2007.

[15] S. Aribo, S. J. Olusegun, L. J. Ibhadiyi, A. Oyetunji, and D. O. Folorunso, "Green inhibitors for corrosion protection in acidizing oilfield environment," *Journal of the Association of Arab Universities for Basic and Applied Sciences*, vol. 24, no. 1, pp. 34–38, 2017.

[16] R. Salghi, S. Jodeh, E. E. Ebenso et al., "6-Phenylpyridazin-3 (2H) one as new corrosion inhibitor for C38 steel in 1 M HCl," *Internetional Journal of Electrochemical Science*, pp. 3309–3322, 2017.

[17] K. K. Alaneme, S. J. Olusegun, and O. T. Adelowo, "Corrosion inhibition and adsorption mechanism studies of hunteria umbellata seed husk extracts on mild steel immersed in acidic solutions," *Alexandria Engineering Journal*, vol. 55, no. 1, pp. 673–681, 2016.

[18] E. Ituen, A. James, O. Akaranta, and S. Sun, "Eco-friendly corrosion inhibitor from Pennisetum purpureum biomass and synergistic intensifiers for mild steel," *Chinese Journal of Chemical Engineering*, vol. 24, no. 10, pp. 1442–1447, 2016.

[19] L. Afia, R. Salghi, L. Bammou et al., "Anti-corrosive properties of Argan oil on C38 steel in molar HCl solution," *Journal of Saudi Chemical Society*, vol. 18, no. 1, pp. 19–25, 2014.

[20] Y. Qiang, S. Zhang, B. Tan, and S. Chen, "Evaluation of Ginkgo leaf extract as an eco-friendly corrosion inhibitor of X70 steel in HCl solution," *Corrosion Science*, vol. 133, pp. 6–16, 2018.

[21] P. Li, D. Chen, Y. Shi, and X. Li, "Evaluation of ficus tikoua leaves extract as an eco-friendly corrosion inhibitor for carbon steel in HCl media," *Biochemistry*, Vol. 128, pp. 49–55, 2019.

[22] E. A. Noor, "Temperature effects on the corrosion inhibition of mild steel in acidic solutions by aqueous extract of fenugreek leaves," *International Journal of Electrochemical Science*, vol. 2, no. 12, pp. 996–1017, 2007.

[23] Q. Ghazali and N. H. M. Yasin, "The effect of organic solvent, temperature and mixing time on the production of oil from moringa oleifera seeds," *Earth and Environmental Science*, 2016.

[24] J. Aljourani, K. Raeissi, and M. A. Golozar, "Benzimidazole and its derivatives as corrosion inhibitors for mild steel in 1M HCl solution," *Corrosion Science*, vol. 51, no. 8, pp. 1836–1843, 2009.

[25] V. V. Torres, R. S. Amado, C. F. de Sá et al., "Inhibitory action of aqueous coffee ground extracts on the corrosion of carbon steel in HCl solution," *Corrosion Science*, vol. 53, no. 7, pp. 2385–2392, 2011.

[26] M. G. Tsoeunyane, M. E. Makhatha, and O. A. Arotiba, "Corrosion inhibition of mild steel by poly (butylene succinate)-L-histidine extended with 1,6-diisocynatohexane polymer composite in 1 M HCl," *International Journal of Corrosion*, vol. 2019, Article ID 7406409, 12 pages, 2019.

[27] Y. Qiang, S. Zhang, B. Tan, and S. Chen, "Evaluation of Ginkgo leaf extract as an eco-friendly corrosion inhibitor of X70 steel in HCl solution," *Corrosion Science*, vol. 133, pp. 6–16, 2018.

[28] A. Bousskri, A. Anejjar, M. Messali et al., "Corrosion inhibition of carbon steel in aggressive acidic media with 1-(2-(4-chlorophenyl)-2-oxoethyl)pyridazinium bromide," *Journal of Molecular Liquids*, vol. 212, pp. 1000–1008, 2015.

[29] I. Ukpong, O. Bamgboye, and O. Soriyan, "Synergistic inhibition of mild steel corrosion in seawater and acidic medium by cathodic protection and monodora myristica using zinc anode," *International Journal Corrosion*, vol. 2018, 8 pages, 2018.

[30] A. Khadiri, R. Saddik, K. Bekkouche et al., "Gravimetric, electrochemical and quantum chemical studies of some pyridazine derivatives as corrosion inhibitors for mild steel in 1 M HCl solution," *Journal of the Taiwan Institute Chemical Engineers*, vol. 58, pp. 552–564, 2016.

[31] G. Weinan, X. Bin, Y. Xiaoshuang, L. Ying, C. Yun, and Y. Wenzhong, "Halogen-substituted thiazole derivatives as corrosion inhibitors for mild steel in 0.5 M sulfuric acid at high temperature," *Journal of the Taiwan Institute Chemical Engineers*, vol. 97, pp. 466–479, 2019.

[32] K. A. A. Al-sodani, O. S. B. Al-amoudi, M. Maslehuddin, and M. Shameem, "Efficiency of corrosion inhibitors in mitigating corrosion of steel under elevated temperature and chloride

concentration," *Construction and Building Materials*, vol. 163, pp. 97–112, 2018.

[33] J. Zhang, L. Zhang, and G. Tao, "A novel and high-efficiency inhibitor of 5-(4-methoxyphenyl)-3h-1,2-dithiole-3-thione for copper corrosion inhibition in sulfuric acid at different temperatures," *Journal of Molecular Liquids*, vol. 272, pp. 369–379

[34] O. Sanni, A. P. I. Popoola, and O. S. I. Fayomi, "Enhanced corrosion resistance of stainless steel type 316 in sulphuric acid solution using eco-friendly waste product," *Results in Physics*, vol. 9, pp. 225–230, 2018.

[35] N. Chaubey, V. Kumar, and M. A. Quraishi, "Corrosion inhibition performance of different bark extracts on aluminium in alkaline solution," *Journal of the Association of Arab Universities for Basic and Applied Sciences*, vol. 22, no. 1, pp. 38–44, 2017.

[36] N. El Hamdani, R. Fdil, M. Tourabi, C. Jama, and F. Bentiss, "Alkaloids extract of *Retama monosperma* (L.) boiss. seeds used as novel eco-friendly inhibitor for carbon steel corrosion in 1 M HCl solution: electrochemical and surface studies," *Applied Surface Science*, vol. 357, pp. 1294–1305, 2015.

[37] A. Farahi, F. Bentiss, C. Jama, M. A. El Mhammedi, and M. Bakasse, "A new approach in modifying ethylene glycol methacrylate phosphate coating formulation by adding sodium montmorillonite to increase corrosion resistance properties," *Journal of Alloys and Compounds*, vol. 723, pp. 1032–1038, 2017.

[38] P. Muthukrishnan, P. Prakash, B. Jeyaprabha, and K. Shankar, "Stigmasterol extracted from Ficus hispida leaves as a green inhibitor for the mild steel corrosion in 1M HCl solution," *Arabian Journal of Chemistry*, 2015.

[39] P. Arellanes-Lozada, O. Olivares-Xometl, N. V. Likhanova, I. V. Lijanova, J. R. Vargas-García, and R. E. Hernández-Ramírez, "Adsorption and performance of ammonium-based ionic liquids as corrosion inhibitors of steel," *Journal of Molecular Liquids*, vol. 265, pp. 151–163, 2018.

[40] R. Solmaz, "Investigation of the inhibition effect of 5-((E) -4-phenylbuta-1, 3-dienylideneamino)-1, 3, 4-thiadiazole-2-thiol Schiff base on mild steel corrosion in hydrochloric acid," *Corrosion Science*, vol. 52, no. 10, pp. 3321–3330, 2010.

[41] A. El jaouhari, S. Kaya, S. Ben jadi et al., "Experimental and MDS studies of corrosion inhibition of carbon steel by saccharinate sodium," *Surfaces and Interfaces*, vol. 10, pp. 11–18, 2018.

[42] C. da Rocha, J. A. da Cunha Ponciano Gomes, and D.'E. Elia, "Corrosion inhibition of carbon steel in hydrochloric acid solution by fruit peel aqueous extracts," *Corrosion Science*, vol. 52, no. 7, pp. 2341–2348, 2010.

[43] K. Al Mamari, H. Elmsellem, N. K. Sebbar et al., "Electrochemical and theoretical quantum approaches on the inhibition of mild steel corrosion in HCl using synthesized benzothiazine compound," *Journal of Materials and Environmental Science*, 2016.

[44] M. Cui, S. Ren, H. Zhao, L. Wang, and Q. Xue, "Novel nitrogen doped carbon dots for corrosion inhibition of carbon steel in 1 M HCl solution," *Applied Surface Science*, vol. 443, pp. 145–156, 2018.

[45] H. Hamani, T. Douadi, D. Daoud, M. Al-Noaimi, and S. Chafaa, "Corrosion inhibition efficiency and adsorption behavior of azomethine compounds at mild steel/hydrochloric acid interface," *Journal of the Measurement Confederation*, vol. 94, pp. 837–846, 2016.

[46] C. Wang, J. Chen, J. Han, C. Wang, and B. Hu, "Enhanced corrosion inhibition performance of novel modified polyaspartic acid on carbon steel in HCl solution," *Journal of Alloys and Compounds*, vol. 771, pp. 736–746, 2019.

[47] M. Faustin, A. Maciuk, P. Salvin, C. Roos, and M. Lebrini, "Corrosion inhibition of C38 steel by alkaloids extract of Geissospermum laeve in 1 M hydrochloric acid : electrochemical and phytochemical studies," *Corrosion Science*, vol. 92, pp. 287–300, 2014.

[48] M. Faustin, A. Maciuk, P. Salvin, C. Roos, and M. Lebrini, "Corrosion inhibition of C38 steel by alkaloids extract of Geissospermum laeve in 1 M hydrochloric acid: Electrochemical and phytochemical studies," *Corrosion Science*, vol. 92, pp. 287–300, 2015.

[49] N. Anusuya, J. Saranya, and P. Sounthari, "Corrosion inhibition and adsorption behaviour of some bis-pyrimidine derivatives on mild steel in acidic medium," *Journal of Molecular Liquids*, vol. 225, pp. 406–417, 2017.

[50] R. Salghi, S. Jodeh, E. E. Ebenso et al., "Benchat, 6-phenylpyridazin-3 (2H) one as new corrosion inhibitor for C38 steel in 1 M HCl," *International Journal of Electrochemical Science*, vol. 12, pp. 3309–3322, 2017.

[51] I. M. Alwaan, "Experimental and Runge–Kutta method simulation to investigate corrosion kinetics of mild steel in sulfuric acid solutions," *International Journal of Corrosion*, vol. 2018, pp. 1–6, 2018.

[52] S. Dahiya, S. Lata, R. Kumar, and O. S. Yadav, "Comparative performance of Uroniums for controlling corrosion of steel with methodical mechanism of inhibition in acidic medium: part1," *Journal of Molecular Liquids*, vol. 221, pp. 124–132, 2016.

[53] J. Bhawsar, P. K. Jain, and P. Jain, "Experimental and computational studies of *Nicotiana tabacum* leaves extract as green corrosion inhibitor for mild steel in acidic medium," *Alexandria Engineering Journal*, vol. 54, no. 3, pp. 769–775, 2015.

[54] S. A. Ali, A. J. Hamdan, A. A. Al-Taq, S. M. J. Zaidi, and M. T. Saeed, "In search of functionality for efficient inhibition of mild steel corrosion both in HCl and H_2SO_4," *Corrosion Engineering Science Technology*, vol. 46, no. 7, pp. 796–806, 2011.

[55] A. Ghazoui, N. Benchat, F. El-Hajjaji et al., "The study of the effect of ethyl (6-methyl-3-oxopyridazin-2-yl) acetate on mild steel corrosion in 1M HCl," *Journal of Alloys and Compounds*, vol. 693, pp. 510–517, 2017.

[56] D. Hmamou, R. Salghi, A. Zarrouk et al., "Carob seed oil : an efficient inhibitor of C38 steel corrosion in hydrochloric acid," *International Journal of Industrial Chemistry*, vol. 3, pp. 1–25, 2012.

[57] A. S. Yaro, A. A. Khadom, and R. K. Wael, "Apricot juice as green corrosion inhibitor of mild steel in phosphoric acid," *Alexandria Engineering Journal*, vol. 52, no. 1, pp. 129–135, 2013.

[58] N. Chaubey, V. K. Savita Singh, and M. Quraishi, "Corrosion inhibition performance of different bark extracts on aluminium in alkaline solution," *Journal of the Association of Arab Universities for Basic and Applied Sciences*, vol. 22, no. 1, pp. 38–44, 2017.

[59] A. Fawzy, M. Abdallah, I. A. Zaafarany, S. A. Ahmed, and I. I. Althagafi, "NU SC," *Journal of Molecular Liquids*, vol. 2017, 2018.

[60] M. Mobin, R. Aslam, and J. Aslam, "Non toxic biodegradable cationic gemini surfactants as novel corrosion inhibitor for mild steel in hydrochloric acid medium and synergistic effect of sodium salicylate : experimental and theoretical approach," *Materials Chemistry Physics*, vol. 191, pp. 151–167, 2017.

[61] R. Karthikaiselvi and S. Subhashini, "Study of adsorption properties and inhibition of mild steel corrosion in hydrochloric acid media by water soluble composite poly (vinyl alcohol-o-methoxy aniline)," *Journal of the Association of Arab Universities for Basic and Applied Sciences*, vol. 16, no. 1, pp. 74–82, 2014.

[62] E. Baran, A. Cakir, and B. Yazici, "Inhibitory effect of gentiana olivieri extracts on the corrosion of mild steel in 0.5M HCl: electrochemical and phytochemical evaluation," *Arabian Journal of Chemistry*, 2016.

[63] L. Bammou, M. Belkhaouda, R. Salghi et al., "Corrosion inhibition of steel in sulfuric acidic solution by the *Chenopodium ambrosioides* extracts," *Journal of the Association of Arab Universities for Basic and Applied Sciences*, vol. 16, pp. 83–90, 2014.

[64] E. Ech-Chihbi, R. Salim, H. Oudda et al., "Experimental and computational studies on the inhibition performance of the organic compound '2-phenylimidazo [1,2-a]pyrimidine-3-carbaldehyde' against the corrosion of carbon steel in 1.0 M HCl solution," *Surfaces and Interfaces*, vol. 9, pp. 206–217, 2017.

[65] N. Anusuya, J. Saranya, P. Sounthari, A. Zarrouk, and S. Chitra, "Corrosion inhibition and adsorption behaviour of some bis-pyrimidine derivatives on mild steel in acidic medium," *Journal of Molecular Liquids*, vol. 225, pp. 406–417, 2017.

[66] X. Li, S. Deng, and H. Fu, "Inhibition of the corrosion of steel in HCl, H_2SO_4 solutions by bamboo leaf extract," *Corrosion Science*, vol. 62, pp. 163–175, 2012.

[67] S. A. Umoren, M. M. Solomon, I. B. Obot, and R. K. Suleiman, "A critical review on the recent studies on plant biomaterials as corrosion inhibitors for industrial metals," *Journal of Industrial and Engineering Chemistry*, vol. 76, pp. 91–115, 2019.

[68] R. F. B. Cordeiro, A. J. S. Belati, D. Perrone, and E. D. Elia, "Coffee husk as corrosion inhibitor for mild steel in HCL media," *International Journal of Electrochemical Science*, vol. 13, pp. 12188–12207, 2018.

[69] B. D. A. Ripper, D. Perrone, C. De Tecnologia, and R. De Janeiro, "Roasted coffee extracts as corrosion inhibitors for mild steel in HCL solution," *Materials Research*, vol. 19, no. 6, pp. 1276–1285, 2016.